NMR Mapping of the HIV-1 Tat Interaction Surface of the KIX Domain of the Human Coactivator CBP†

Andrew C. Vendel and Kevin J. Lumb*

Department of Biochemistry and Molecular Biology, Colorado State University, Fort Collins, Colorado 80523-1870

Received September 7, 2003; Revised Manuscript Received November 23, 2003

ABSTRACT: Tat is required for the expression of the HIV-1 genome. HIV-1 Tat interacts with the human transcriptional coactivator and acetyltransferase CREB-binding protein (CBP) via the KIX domain of CBP. Chemical shift perturbation mapping with nuclear magnetic resonance spectroscopy was used to identify the surface of human KIX that interacts with Tat. It was found that Tat binds to the c-Jun/MLL/Tax binding surface of KIX, as opposed to the CREB binding site. The results provide new insight into the molecular basis of the assembly of protein complexes involving p300/CBP and Tat during HIV gene expression.

Expression of the HIV genome requires both viral and human proteins (*1*, *2*). Viral transcription initiation is mediated by endogenous human transcriptional activators such as NF-κB and SP-1, which presumably contribute to the recruitment of the general transcription machinery to the viral promoter (*1*, *2*). Efficient elongation, however, requires the HIV-1[1] transcriptional activator Tat (*1*, *2*). Tat binds the nascent transcribed viral RNA and interacts with a number of host transcription factors (*1*, *2*). For example, Tat recruits pTEFb (cyclin T1-Cdk9), which phosphorylates the C-terminal domain of RNA polymerase II to promote transcription elongation (*2*).

The human transcriptional coactivator and acetyltransferase CBP and the highly related but distinct p300 contribute to gene expression during cellular processes such as cell growth, differentiation, and tumor progression (*3*, *4*). In addition to the acetyltransferase domain, CBP and p300 contain several autonomously functional protein−protein interaction domains that bind a large number of transcription factors (*3*, *4*). The acetyltransferase activity and ability to mediate numerous protein−protein interactions suggest that CBP and p300 contribute to transcription via assembly of the transcription machinery and through nucleosome remodeling (*3*, *4*).

A bevy of recent reports points to an important functional relationship between Tat and p300/CBP during HIV gene expression. Tat interacts with the acetyltransferase and KIX domains of p300/CBP and with the bromo domain of the p300/CBP-associated factor PCAF (*5*−*10*). Tat can also be acetylated by p300, CBP, and PCAF (*8*, *11*−*13*), and Tat is implicated in the p300/CBP-mediated acetylation of histone H4 and NF-κB (*14*−*16*). In addition, human transcription factors involved in HIV-1 gene expression also bind p300/CBP (*3*, *4*) and perhaps act in concert with Tat to recruit p300/CBP during assembly of the transcription enhanceosome.

The KIX domain of p300/CBP binds several cellular and viral transcription factors (*3*, *4*) via two discrete modes that employ structurally distinct surfaces of KIX (*17*−*21*). One mode is represented by the phosphorylation-induced binding of the KID region of CREB to KIX (*17*). c-Myb also binds constitutively to a similar region of KIX as phosphorylated KID (*20*). The second mode is exemplified by the human transcription factors c-Jun and MLL and by the viral transcriptional activator HTLV-1 Tax, which bind constitutively to a different surface of KIX than phosphorylated KID (*18*, *19*, *21*).

We have demonstrated previously that Tat binds directly to the KIX domain of p300/CBP in vitro and that KIX interferes with Tat-mediated transcription in human T cells (*10*). The interaction is localized to the N-terminal 24 residues of Tat, with Tat_{1-24}, corresponding to the N-terminal 24 residues of HXB2 isolate Tat, forming a specific complex with KIX (*10*). Here we extend our previous studies of the Tat−KIX complex by identifying the Tat_{1-24} binding site on KIX with heteronuclear NMR spectroscopy. Our results show that Tat binds to the c-Jun/MLL/Tax binding surface of KIX, as opposed to the CREB/c-Myb binding site and contribute to our understanding of the molecular basis of the Tat-p300/CBP interaction.

EXPERIMENTAL PROCEDURES

Protein Preparation and Purification. Tat_{1-24}, corresponding to residues 1−24 of HXB2 isolate HIV-1 Tat, was synthesized using manual Boc chemistry and purified with reverse-phase C_{18} HPLC as described previously (*10*). The identity of Tat_{1-24} was confirmed with electrospray mass spectrometry, and the observed and expected masses agreed to within 1 Da.

† Supported by the American Cancer Society (RSG-02-051-GMC).

* Corresponding author. Present address: Bayer Pharmaceutical Corp., 400 Morgan Lane, West Haven, CT 06516. E-mail: kevin.lumb.b@bayer.com.

[1] Abbreviations: CBP, CREB-binding protein; CREB, cyclic AMP response element binding protein; DSS, sodium 2,2-dimethyl-2-silapentane-5-sulfonate; HPLC, high-performance liquid chromatography; HSQC, heteronuclear single-quantum coherence; HIV-1, human immunodeficiency virus type 1; KID, kinase-inducible domain of CREB; KIX, KID-interacting domain of CBP; MLL, mixed lineage leukemia protein; NMR, nuclear magnetic resonance; PCAF, p300/CBP-associated factor; ppm, parts per million.

10.1021/bi035612l CCC: $27.50
Published on Web 01/08/2004

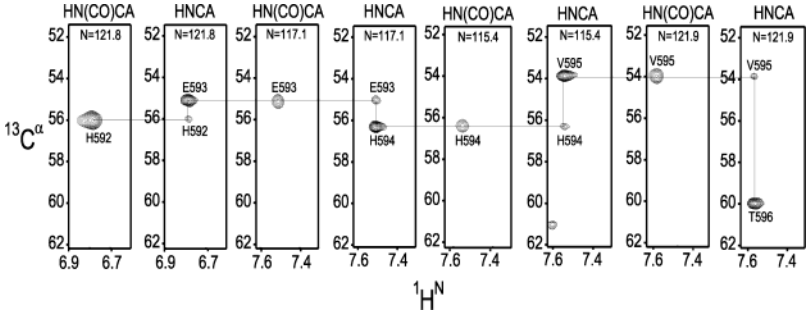

FIGURE 1: Detail of the HNCA and HN(CO)CA spectra showing sequential and intraresidue connectivities used to assign the resonances of His 592 to Thr 596 of KIX in the Tat_{1-24}−KIX complex (10 °C, pH 7).

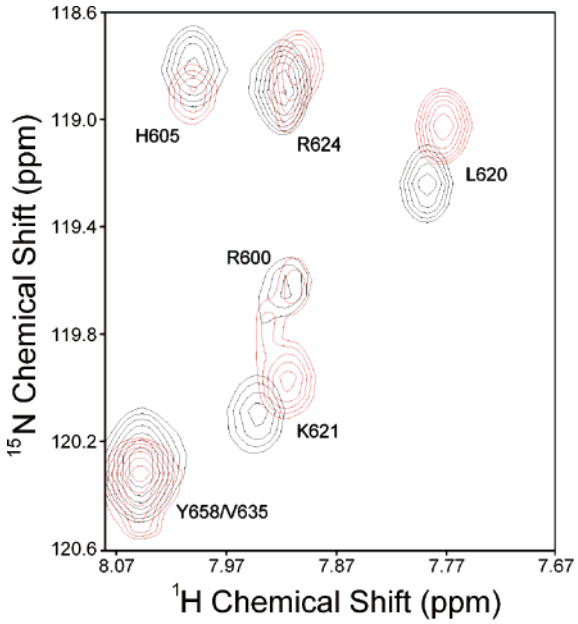

FIGURE 2: Detail of the $^{1}H-^{15}N$ HSQC spectrum of ^{15}N-labeled KIX showing changes in KIX chemical shifts upon binding Tat_{1-24} (10 °C, pH 7). Resonances of free KIX and Tat_{1-24}-bound KIX are shown in black and red, respectively.

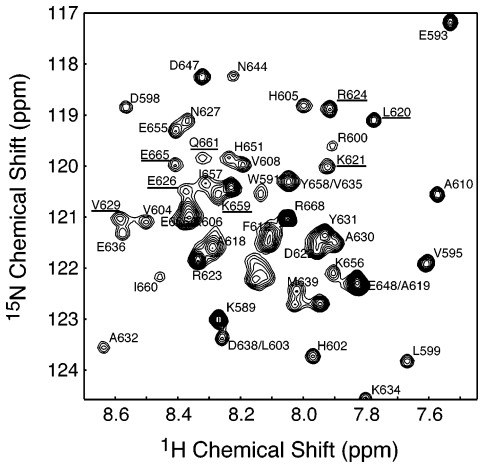

FIGURE 3: $^{1}H-^{15}N$ HSQC spectrum of ^{15}N-labeled KIX bound with Tat_{1-24}. Resonances that have a significant chemical shift change upon binding Tat_{1-24} are underlined.

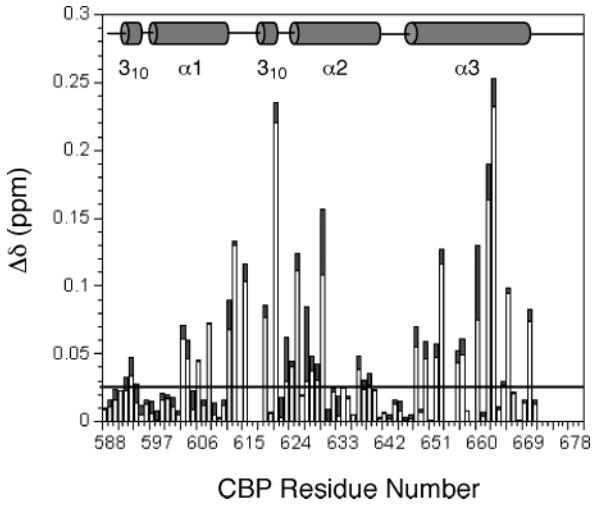

FIGURE 4: Chemical shift changes induced in KIX by Tat_{1-24}. ^{15}N and ^{1}H changes are shown as open and filled bars, respectively. The secondary structure of KIX comprises three α and two 3_{10} helices (*17*) and is shown as a schematic. The horizontal line at 0.03 ppm denotes the average combined change in ^{15}N and ^{1}H chemical shift.

^{15}N and ^{13}C,^{15}N-labeled KIX (residues 589−679 of human CBP with an additional N-terminal Met) was expressed in *Escherichia coli* strain BL21(DE3) pLysS and purified as described previously (*10*). Cells were grown in M9 medium supplemented with thiamine containing $(^{15}NH_4)_2SO_4$ and/or [^{13}C]glucose as the sole nitrogen and carbon sources, respectively (*22*). Final purification was by reversed-phase C_{18} HPLC. The identity of KIX was confirmed with electrospray mass spectrometry, and the observed and expected masses agreed to within 1 Da.

Protein Concentration Determination. Concentrations of protein stock solutions used to prepare NMR samples were determined by absorbance in 6 M GuHCl, 10 mM sodium phosphate, and 150 mM sodium chloride, pH 6.5 at 25 °C (*23*). Extinction coefficients at 280 nm for KIX and Tat_{1-24} of 12090 and 5690 M^{-1} cm^{-1} were used, respectively.

NMR Spectroscopy. NMR spectra were acquired with a Varian Unity Inova operating at 500.1 MHz for ^{1}H and referenced to internal DSS at zero ppm. Data were processed with NMRPipe and analyzed with NMRView (*24*, *25*). All spectra were acquired at 10 °C on samples prepared in 10 mM sodium phosphate and 150 mM NaCl, pH 7.0.

Gradient sensitivity-enhanced HNCA and HN(CO)CA spectra (*26*−*28*) were collected with 16 transients per increment. Spectra comprised 1024, 64, and 32 complex points in the ^{1}H, ^{13}C, and ^{15}N dimensions, respectively. Data were resolution enhanced and zero filled once prior to Fourier transformation. Samples contained 600 μM ^{13}C,^{15}N-labeled KIX and 2 mM Tat_{1-24}.

Gradient $^{1}H-^{15}N$ HSQC spectra (*29*) consisted of 256 complex increments defined by 128 transients and 1024 complex points. Data were resolution enhanced and zero

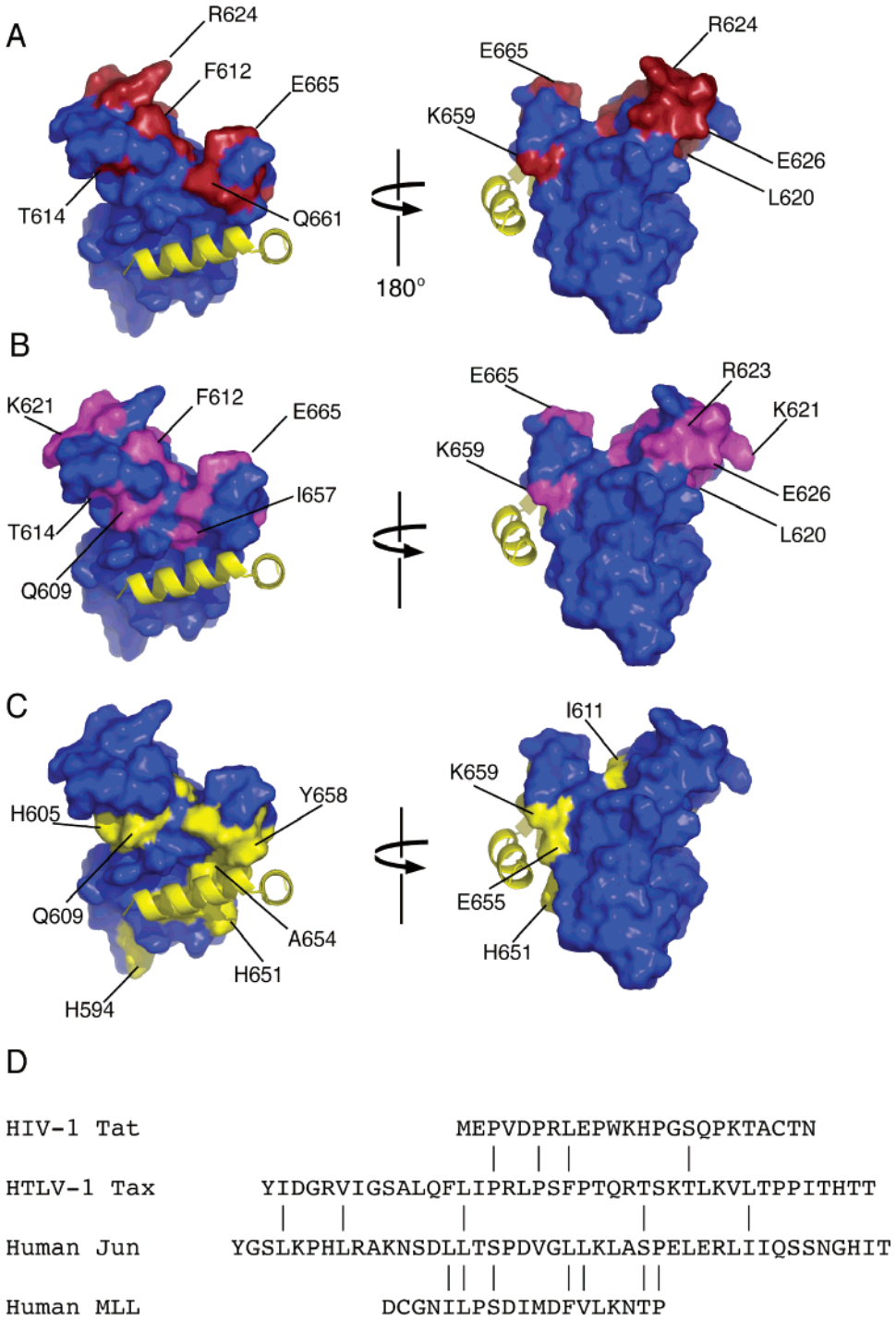

FIGURE 5: (A) Chemical shift perturbation mapping of the Tat binding site. (B) Chemical shift perturbation mapping of the Jun binding site, as reported previously (*18*). (C) Chemical shift perturbation mapping of the CREB binding site, as reported previously (*18*, *31*). Regions of KIX that experience significant chemical shift changes upon binding Tat, c-Jun (*18*), and CREB (*17*, *18*) are shown in red, purple, and yellow, respectively. Regions of KIX that are unaffected by binding are shown in blue. The KID region of CREB is shown as a yellow ribbon. (D) Sequence alignments of the KIX-interacting regions of HIV-1 Tat (*10*), HTLV-1 Tax (*21*), human c-Jun (*18*), and human MLL (*19*). c-Jun and MLL share some sequence similarity. However, meaningful sequence similarity or a common sequence motif between Tat and the two human proteins is not apparent. Figures created with the PDB file 1kdx (*31*) and PyMOL (*35*).

filled once prior to Fourier transformation to give a final digital resolution of 3 and 4 Hz/point in the ^{1}H and ^{15}N dimensions, respectively. Samples contained 225 μM ^{15}N-labeled KIX or 225 μM ^{15}N-labeled KIX and 550 μM Tat_{1-24}.

RESULTS AND DISCUSSION

We have shown previously that Tat interacts with the KIX domain of CBP in vitro and that KIX interferes with Tat-mediated transcription from the HIV-1 promoter in human T cells (*10*). Tat is intrinsically disordered in isolation and may fold to a helical structure upon binding KIX (*10*). Here we further define the interaction between Tat and CBP with NMR chemical shift perturbation mapping (*30*) to identify the Tat binding surface on KIX.

It is generally not possible to ascribe changes in chemical shift to specific conformational changes due to the multifari-

ous contributions to the chemical shift (*30*). Nonetheless, the recognition interface may be mapped by chemical shift changes upon complex formation if the perturbed residues form a contiguous surface of the bound protein (*30*). For example, chemical shift mapping identified correctly the CREB binding site on KIX known from a structural determination of the pKID−KIX complex and was used to map the KIX interaction surfaces of c-Jun, MLL, c-Myb, and HTLV-1 Tax (*18*−*20*, *31*).

The NMR assignments of $^{13}C,^{15}N$-labeled KIX bound with Tat_{1-24} were obtained directly from HNCA and HN(CO)-CA spectra (Figure 1). Assignments were obtained for 75 residues of KIX in the complex from an expected total of 90 (94 residues minus three Pro residues and Met 1). Changes in the ^{1}H and ^{15}N chemical shifts of KIX were then obtained with greater precision from gradient $^{1}H-^{15}N$ HSQC spectra of ^{15}N-labeled KIX bound with unlabeled Tat_{1-24} (Figures 2 and 3) to obtain the changes in chemical shift of KIX resonances upon binding Tat_{1-24} (Figure 4).

The largest chemical shift perturbations induced in KIX upon binding Tat_{1-24} are seen for F612, T614, L620, D622, R624, E626, V629, K659, Q661, K662, and E665 (Figure 4). The changes in ^{1}H and ^{15}N chemical shifts of these residues are at least 2-fold greater than the average chemical shift change of 0.01 for ^{1}H and 0.04 ppm for ^{15}N. The residues form a contiguous surface of KIX that contains both hydrophobic and polar residues that defines the Tat binding surface of KIX (Figure 5A).

The Tat binding site of KIX is distinct from the CREB binding site and instead corresponds to the site recognized by c-Jun. The chemical shift changes seen upon binding Tat_{1-24} occur in the same region of KIX as observed upon binding the c-Jun activation domain (Figure 5B) and not at the surface recognized by CREB and c-Myb (Figure 5C). HTLV-1 Tax and human MLL also bind KIX at a similar surface to that occupied by c-Jun (*19*, *21*). The chemical shift perturbations of KIX induced by Tat_{1-24} are somewhat smaller than the changes caused by the c-Jun and MLL activation domains (*18*, *19*) but map to the same surface of KIX as those induced by c-Jun (Figure 5). We conclude that HIV-1 Tat, HTLV-1 Tax, human c-Jun, and human MLL recognize a common binding surface of KIX.

Although HIV-1 Tat, HTLV-1 Tax, human c-Jun, and human MLL bind the same surface of KIX, the sequence similarity between the KIX-interacting regions of Tat and human c-Jun or MLL is insignificant (Figure 5D). The KIX-interacting regions of human c-Jun and MLL share a higher degree of sequence similarity (Figure 5D) but do not share an obvious common sequence motif with Tat (Figure 5D). Tat also shares very limited sequence identity with HTLV-1 Tax (Figure 5D), which also occupies the same site as Tat (*21*). As noted previously (*21*), high-resolution structures are required to determine whether quaternary interactions with KIX impart a common structural motif to the transcriptional activators that occupy that the Tat/Tax/Jun/MLL site or if the activators employ a structurally divergent binding mode for binding KIX.

HIV infection can lead to associated pathogenesis such as Kaposi's sarcoma and non-Hodgkin's lymphoma that are presumably caused, in part, by the deregulation of normal gene expression. Our results imply that the normal functions of transcription factors that use the c-Jun/MLL binding site of KIX binding site may be disrupted directly by the competitive sequestration of p300/CBP by Tat. Since p300/CBP is believed to be present at limiting quantities in the cell (*32*−*34*), sequestration of p300/CBP by Tat may have significant consequences for deregulating cellular processes that depend in part on interactions mediated by the KIX domain during gene expression.

In conclusion, we have used NMR spectroscopy to identify the Tat-interacting surface of the KIX domain of CBP. We find that Tat binds the same site of KIX that recognizes c-Jun and MLL, which is distinct from the site used by CREB and c-Myb. The results provide new insight into the molecular basis of the assembly of protein complexes involving p300/CBP and Tat during HIV gene expression and provide a rational framework for future structure−function studies of the Tat-p300/CBP interaction.

ACKNOWLEDGMENT

We thank Drs. K. M. Campbell and C. D. Rithner for helpful discussions.

REFERENCES

1. Jones, K. A., and Peterlin, B. M. (1994) *Annu. Rev. Biochem. 63*, 717−743.
2. Karn, J. (1999) *J. Mol. Biol. 293*, 235−254.
3. Goodman, R. H., and Smolik, S. (2000) *Genes Dev. 14*, 1553−1577.
4. Chan, H. M., and La Thangue, N. B. (2001) *J. Cell Sci. 114*, 2363−2373.
5. Benkirane, M., Chun, R. F., Xiao, H., Ogryzko, V. V., Howard, B. H., Nakatani, Y., and Jeang, K. T. (1998) *J. Biol. Chem. 273*, 24898−24905.
6. Hottiger, M. O., and Nabel, G. J. (1998) *J. Virol. 72*, 8252−8256.
7. Marzio, G., Tyagi, M., Gutierrez, M. I., and Giacca, M. (1998) *Proc. Natl. Acad. Sci. U.S.A. 95*, 13519−13524.
8. Deng, L., de la Fuente, C., Fu, P., Wang, L., Donnelly, R., Wade, J. D., Lambert, P., Li, H., Lee, C., and Kashanchi, F. (2000) *Virology 277*, 278−295.
9. Mujtaba, S., He, Y., Zeng, L., Farooq, A., Carlson, J. E., Ott, M., Verdin, E., and Zhou, M. M. (2002) *Mol. Cell 9*, 575−586.
10. Vendel, A., C., and Lumb, K. J. (2003) *Biochemistry 42*, 910−916.
11. Kiernan, R. E., Vanhulle, C., Schiltz, L., Adam, E., Xiao, H., Maudoux, F., Calomme, C., Burny, A., Nakatani, Y., Jeang, K. T., Benkirane, M., and Van Lint, C. (1999) *EMBO J. 18*, 6106−6118.
12. Ott, M., Schnolzer, M., Garnica, J., Fischle, W., Emiliani, S., Rackwitz, H. R., and Verdin, E. (1999) *Curr. Biol. 9*, 1489−1492.
13. Kaehicke, K., Dorr, A., Hetzer-Egger, C., KIiermer, V., Henklein, P., Schnoelzer, M., Loret, E., Cole, P. A., Verdin, E., and Ott, M. (2003) *Mol. Cell 12*, 167−176.
14. Deng, L., Wang, D., de la Fuente, C., Wang, L., Li, H., Lee, C. G., Donnelly, R., Wade, J. D., Lambert, P., and Kashanchi, F. (2001) *Virology 289*, 312−326.
15. Col, E., Gilquin, B., Caron, C., and Khochbin, S. (2002) *J. Biol. Chem. 277*, 37955−37960.
16. Furia, B., Deng, L., Wu, K., Baylor, S., Kehn, K., Li, H., Donnelly, R., Coleman, T., and Kashanchi, F. (2002) *J. Biol. Chem. 277*, 4973−4980.
17. Radhakrishnan, I., Pérez-Alvarado, G. C., Parker, D., Dyson, H. J., Montminy, M. R., and Wright, P. E. (1997) *Cell 91*, 741−752.
18. Campbell, K. M., and Lumb, K. J. (2002) *Biochemistry 41*, 13956−13964.
19. Goto, N. K., Zor, T., Martinez-Yamout, M., Dyson, H. J., and Wright, P. E. (2002) *J. Biol. Chem. 277*, 43168−43174.
20. Zor, T., Mayr, B. M., Dyson, H. J., Montminy, M. R., and Wright, P. E. (2002) *J. Biol. Chem. 277*, 42241−42248.
21. Vendel, A., C., McBryant, S. J., and Lumb, K. J. (2003) *Biochemistry 42*, 12481−12487.

22. McIntosh, L. P., and Dahlquist, F. W. (1990) *Q. Rev. Biophys. 23*, 1−38.
23. Edelhoch, H. (1967) *Biochemistry 6*, 1948−1954.
24. Johnson, B. A., and Blevins, R. A. (1994) *J. Biomol. NMR 4*, 603−614.
25. Delaglio, F., Grzesiek, S., Vuister, G. W., Zhu, G., Pfeifer, J., and Bax, A. (1995) *J. Biomol. NMR 6*, 277−293.
26. Ikura, M., Kay, L. E., and Bax, A. (1990) *Biochemistry 29*, 4659−4667.
27. Bax, A., and Ikura, M. (1991) *J. Biomol. NMR 1*, 99−104.
28. Kay, L. E., Xu, G. Y., and Yamazaki, T. (1994) *J. Magn. Reson. A109*, 129−133.
29. Kay, L., Keifer, P., and Saarinen, T. (1992) *J. Am. Chem. Soc. 114*, 10663−10665.
30. Zuiderweg, E. R. P. (2002) *Biochemistry 41*, 1−7.
31. Radhakrishnan, I., Pérez-Alvarado, G. C., Parker, D., Dyson, H. J., Montminy, M., and Wright, P. E. (1999) *J. Mol. Biol. 287*, 859−865.
32. Kamei, Y., Xu, L., Heinzel, T., Torchia, J., Kurokawa, R., Gloss, B., Lin, S. C., Heyman, R. A., Rose, D. W., Glass, C. K., and Rosenfeld, M. G. (1996) *Cell 85*, 403−414.
33. Horvai, A. E., Xu, L., Korzus, E., Brard, G., Kalafus, D., Mullen, T. M., Rose, D. W., Rosenfeld, M. G., and Glass, C. K. (1997) *Proc. Natl. Acad. Sci. U.S.A. 94*, 1074−1079.
34. Hottiger, M. O., Felzien, L K., and Nabel, G. J. (1998) *EMBO J. 17*, 3124−3134.
35. DeLano, W. L. http://www.pymol.org.

BI035612L